

Impacts of Respiratory Activities on Infection Risk of COVID-19 in a Passenger Elevator

Chengbo Du¹, Qingyan Chen^{2*}

¹School of Mechanical Engineering, Purdue University, West Lafayette, IN 47907, USA

²Department of Building Environment and Energy Engineering, The Hong Kong Polytechnic University, Kowloon, Hong Kong

Abstract. Contaminant transport and flow distribution are very important during an elevator ride, as the reduced social distancing may increase the infection rate of airborne diseases such as COVID-19. This investigation used a computational fluid dynamics (CFD) model based on the RNG $k-\epsilon$ turbulence model to predict airflow and particle transport in an elevator-lobby area with moving passengers. The CFD results showed a complex airflow pattern due to the downwash air supply from the ceiling and the upward thermal plumes generated by passengers. This investigation studied different respiratory activities of the index patient, i.e., breathing, coughing with and without a mask, and speaking. The results quantitatively compare the risk of infection among different respiratory activities. During an elevator ride, the infection risk was generally low because of the short duration. However, if the index patient talked in an elevator, the infection risk would be relatively high, as two passengers in the closest proximity to distance would be infected.

1 Introduction

As a result of the COVID-19 pandemic, more than six million deaths have occurred throughout the world as of May 2022 [1]. One of the main transmission routes of SARS-CoV-2 has been by airborne particles generated by SARS-CoV-2 carriers, according to the Centers for Disease Control and Prevention (CDC) of the United States [2]. Virus transmission during elevator rides has been very concerning, as many people use elevators nearly every day. The high passenger density and closed environment that characterize an elevator ride have facilitated the spread of SARS-CoV-2. Cases of possible COVID-19 transmission in enclosed environments [3,4] such as elevator cabins [5] have been reported. However, although clinical reports have provided evidence of airborne transmission of SARS-CoV-2, very few studies are available for quantitative assessment of infection risk during elevator rides. To evaluate this risk, it is necessary to understand the transmission of virus-laden particles on elevators.

Virus-laden particles can become suspended in the air and can be inhaled by susceptible people [6]. Few studies are available for the transmission of virus-laden particles during elevator rides. Dbouk et al. [15] examined the airflow pattern and airborne transmission in elevators, but they only explored the particle dispersion caused by a stationary index person, and no fellow passengers or body movement was considered. Shao et al. [16] conducted in-situ measurements for respiratory behaviors and implemented the measured

results into a CFD model to investigate the particle transmission in an elevator scenario. However, they did not consider the effects of the wake generated by passengers while entering or exiting the elevator cabin. Also, the infection risk in their study was evaluated in terms of the number of particles passing through a specified location. Liu et al. [17] considered the impact of wake on particle transmission, but they investigated the transmission of airborne particles with breathing activity only.

Therefore, the objectives of this study were (1) to investigate virus-laden particle transmission during an elevator ride and assess the virus exposure of susceptible passengers, and (2) to compare the effects of different respiratory activities on the infection risk for fellow passengers.

2 Method

For consideration of the complex flow pattern resulted from thermal plumes, the ventilation system, and wake by passengers' movement, a reliable analyzer of the fluid field is required. This study employed the Euler-Lagrange approach to calculate particle dispersion. The fluid phase was treated as a continuum and was solved by the Navier-Stokes equations, whereas the virus-laden particles were tracked as a discrete phase separated through the flow domain. One-way coupling was used because the volume fraction of the particle phase is relatively low. Only the fluid phase has momentum and energy impact on the particle phase.

*Corresponding author: qingyan.chen@polyu.edu.hk

2.1 Case description

As shown in Fig. 4, the elevator cabin was 2.00 m long, 1.65 m wide and 2.50 m high. The elevator lobby was 11.50 m long, 5.00 m wide and 4.00 m high. The simplified manikin was 0.40 m × 0.20 m × 1.68 m. The mouth of a manikin is located 223 mm below the head top, with an opening area of 1.2 cm². The temperature setpoint for indoor air was 24 °C. According to ASHRAE standards [25, 26], the ventilation rate of the elevator was 72 ACH (air changes per hour), and the ventilation rate of the lobby was 3 ACH. The inlet of the elevator was a 0.05 m wide slot along the periphery of the elevator ceiling, and the outlet of the elevator was a 0.02 m high slot at the bottom of the walls. Meanwhile, two square ceiling diffusers were used in the lobby. The size of each diffuser was 0.40 m × 0.40 m × 0.03 m, and the direction of the airflow from the diffusers was 15° downward. Since this study considered a relatively large lobby in order to minimize the impact of lobby shape on particle transmission, the outlets of the lobby were the two boundaries along the Y direction, which were connected to the main lobby on the ground floor.

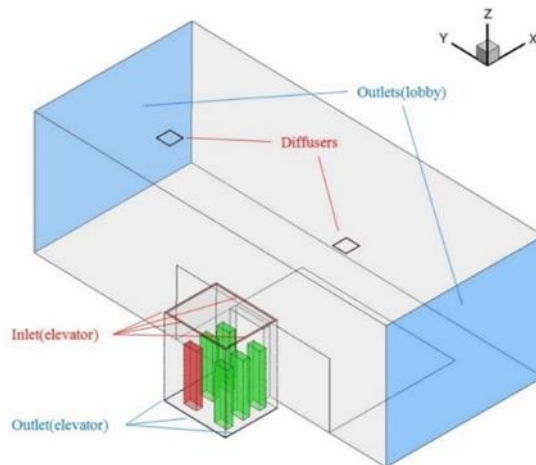


Fig. 1. Geometry a typical elevator-lobby area

Table 1. Boundary conditions in the CFD model

Boundary	Momentum	Thermal	DPM
Inlet (lobby)	2.07 m/s (15° downward)	22°C	Reflect
Inlet (elevator)	0.47 m/s (normal to boundary)	20°C	Reflect
Nose of the index person	User-defined functions	34°C	Reflect
Mouth of the index person	User-defined functions	34°C	Reflect
Outlet (lobby)	Pressure outlet	24°C, backflow	Escape
Outlet (elevator)	Pressure outlet	24°C, backflow	Escape
Susceptible passengers' bodies	No-slip	31°C	Trap
Lobby walls	No-slip	Adiabatic	Trap
Elevator walls	No-slip	Adiabatic	Trap

The corresponding thermo-fluid boundary conditions as well as the discrete phase model (DPM) boundary conditions were described in Table 1.

The interactions of the flow forces would significantly affect the transmission of SARS-CoV-2 among passengers. To comprehensively compare the infection risks during an elevator ride, this study considered four dynamic scenarios, each divided into three sub-cases. The four scenarios are distinguished by the different particle-generation activities of the index passenger: breathing, speaking, uncovered coughing, and covered coughing. All cases included the particles generated by nose breathing. For the sake of simplicity, the cases were named as follows:

- Case 1 - breathing case: only breathing activity was considered;
- Case 2 - uncovered coughing case: both coughing and breathing activities were considered, and no interference was applied to the coughing jet;
- Case 3 - covered coughing case: both coughing and breathing activities were considered, and a surgical mask covered the mouth;
- Case 4 - speaking case: coupled speaking and breathing activities were considered, and the index passenger alternately spoke for 10 seconds and listened for 10 seconds.

Each case was further divided into three sub-cases, namely, 13 seconds for entering the elevator ($t \in [0, 13]$ s), sub-case 1), 120 seconds for riding the elevator ($t \in [13, 133]$ s), sub-case 2), and 13 seconds for leaving the elevator ($t \in [133, 146]$ s), sub-case 3).

2.2 CFD model

To obtain the flow distribution, this study numerically solved unsteady-state Reynolds-averaged Navier-Stokes (RANS) equations with the re-normalization group (RNG) $k-\epsilon$ turbulence model [18]. The governing equations of this turbulence model can be written in a general form as:

$$\frac{\partial(\rho\bar{\Phi})}{\partial t} + \rho\bar{u}_i \frac{\partial\bar{\Phi}}{\partial x_i} - \Gamma_{\phi,eff} \frac{\partial\bar{\Phi}}{\partial x_i} = S_{\phi} \quad (1)$$

where Φ represents the thermo-fluid variables, i.e., velocity, enthalpy, and turbulence parameters such as turbulent kinetic energy and the dissipation rate of the turbulent kinetic energy; $\Gamma_{\phi,eff}$ and S_{ϕ} are the effective diffusion coefficient and the source term for the specific equation, respectively; and u_i and x_i represent the directional components for velocity and space coordinates, respectively [19, 20]. In addition, this study employed the Boussinesq approximation to account for thermal buoyancy.

The Lagrangian method describes the particle trajectory by integrating the force balance on the particle, which is set in a Lagrangian reference frame. As described by Newton's law:

$$\frac{du_p}{dt} = F_D(u - u_p) + \frac{g(\rho_p - \rho)}{\rho_p} \quad (2)$$

where $F_D(u - u_p)$ is the drag force per unit mass, and is defined as:

$$F_D = \frac{18\mu C_D Re}{\rho_p d_p^2 24} \quad (3)$$

Here, Re denotes the relative Reynolds number of particles and is calculated by:

$$Re = \frac{\rho d_p |u_p - u|}{\mu} \quad (4)$$

In these equations, u is the air velocity, u_p is the particle velocity, ρ is the air density, ρ_p is the particle density, μ is the molecular viscosity of air, d_p is the particle diameter, and g is gravitational acceleration.

This study used the discrete random walk (DRW) model to account for the effects of instantaneous turbulent velocity fluctuations on the particle trajectories. A study by Chen et al. [21] has shown the trajectories of a small droplet and its droplet nucleus due to evaporation are almost overlapping. The present study used an inert spherical particle model to simulate the virus-laden particles generated by a person's breathing, coughing and speaking. This study implemented the model by using a commercial CFD software package, ANSYS Fluent version 2020R1.

2.3 Virus-laden particle exhalation and inhalation of different respiratory activities

The size distribution of particles generated by respiratory activities like breathing, coughing, and speaking varies within a wide range, as shown in Table 2. For breathing, Fabian et al. [11] recommended three sizes, 0.4 μm , 0.75 μm and 2.5 μm . For speaking and coughing, a study conducted by Chao et al. [10] used the size classes from 3 μm to 750 μm for both activities. Another study, by Yang et al. [12], revealed that coughing could generate particles that are finer than 3 μm . A study of Yang et al. [12] can be used to obtain the number of particles. Therefore, the present study combined the data from Yang et al. [12] and Chao et al. [10] for the size distribution of particles generated by coughing, and summarized them into Table 2.

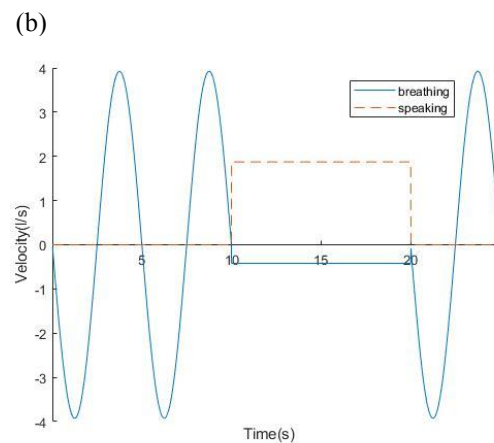
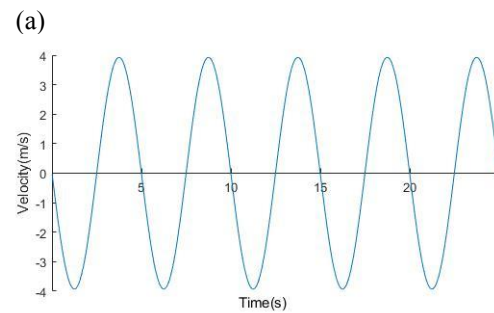
Table 2. Size distribution of particles generated by different activities.

Diameter μm	Number of particles		
	Breathing (Per breath)	Speaking (Per second)	Coughing (Per cough)
0.4	612	N/A	N/A
0.75	156	N/A	140000
1.32	N/A	4	71
2.5	107	N/A	N/A
2.64	N/A	57	974
5.28	N/A	20	362
8.8	N/A	10	119
12.32	N/A	7	44
15.84	N/A	3	42
19.8	N/A	4	36
27.5	N/A	4	36

38.5	N/A	3	25
49.5	N/A	4	30
60.5	N/A	3	28
77	N/A	4	78
99	N/A	3	44
165	N/A	3	37
330	N/A	1	25

Acknowledging that the SARS-CoV-2 virus concentration varies among different body fluids, this study considered saliva and sputum, which are two common virus-laden media released by infected people's noses and mouths. According to an investigation by Pan et al. [13], the SARS-CoV-2 virus concentration in infected people's sputum can be as high as 1.34×10^{11} copies/mL. Meanwhile, To et al. [14] showed that the SARS-CoV-2 virus concentration in saliva was 1.2×10^8 copies/mL.

In addition, since thermo-fluid boundary conditions significantly contribute to particle transmission, this study used detailed flow boundary conditions provided in studies of Gupta et al. [7,9] and Chen et al. [8] which captured the flow characteristics of breathing, speaking, and covered/uncovered coughing cases. For the covered coughing case, it was assumed that the index person was wearing a surgical mask, and the filtration efficiency from Pan et al. [23] was applied. Particles larger than 5.28 μm were all filtered, and the filtration efficiencies for particle sizes of 0.75 μm , 1.32 μm , 2.64 μm and 5.28 μm were 67.3%, 73.0%, 78.0% and 93.0%, respectively. The flow boundary conditions discussed are shown in Fig. 2.



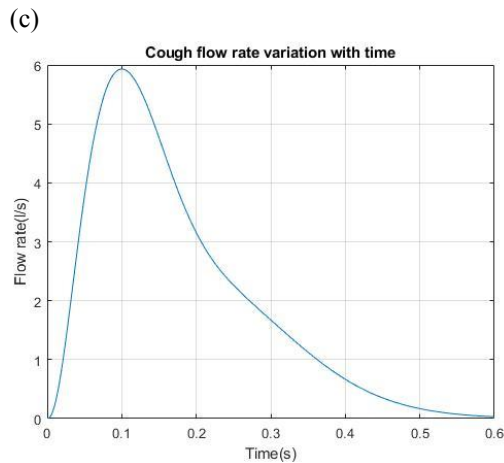


Fig. 2. Flow boundary conditions for particle injection: (a) breathing flow velocity, (b) flow velocity of combined speaking and breathing, (c) flow rate of a single uncovered cough.

The inhalation of virus-laden particles by susceptible passengers is calculated by:

$$Dose_i = \int_0^t \dot{v} \sum_d N_d \cdot \frac{n_{i,d}}{V_i} dt$$

where $n_{i,d}$ is the number of particles with a diameter of d in passenger i 's breathing zone, and V_i is the volume of passenger i 's breathing zone. The breathing zone is defined as a spherical volume centered at a passenger's nose, with a radius of 0.30 m. Meanwhile, \dot{v} is the average breathing flow rate, as $0.00053 \text{ m}^3/\text{s}$, which is consistent with the previous study [30]. The infection risk for susceptible passengers was determined by a threshold of 2,000 accumulative inhaled virus copies [24].

3 Results

3.1 Particle dispersion in an elevator

Fig. 3(a) to (d) show an example of the particle dispersion throughout Case 1. For each breathing period, a total number of 875 particles ranging from $0.4 \mu\text{m}$ to $2.5 \mu\text{m}$ was exhaled. Since the direction of the breathing jet was 60° downward, the particles would first travel down. Next, the thermal plume generated by the passengers' bodies lifted the particles to a higher level. The wake that followed the passengers' movement entrained some particles and brought them along in the direction of the movement. Meanwhile, the circulations generated by the ventilation system played an important role during the two-minute elevator ride. The particles were well mixed and were in a dynamic balance in the elevator cabin within the first 60 seconds. The susceptible passengers in close proximity to the index person faced higher exposure to the particles. The balance was achieved in a short time because of the high air change rate in the elevator cabin.

In the example case, only small particles (with diameters ranging from $0.4 \mu\text{m}$ to $2.5 \mu\text{m}$) were released. However, in the cases where larger particles were released, the large particles ($> 77 \mu\text{m}$) would fall

to the ground very quickly after release. Therefore, susceptible people would be less likely to be exposed to large particles than to small ones.

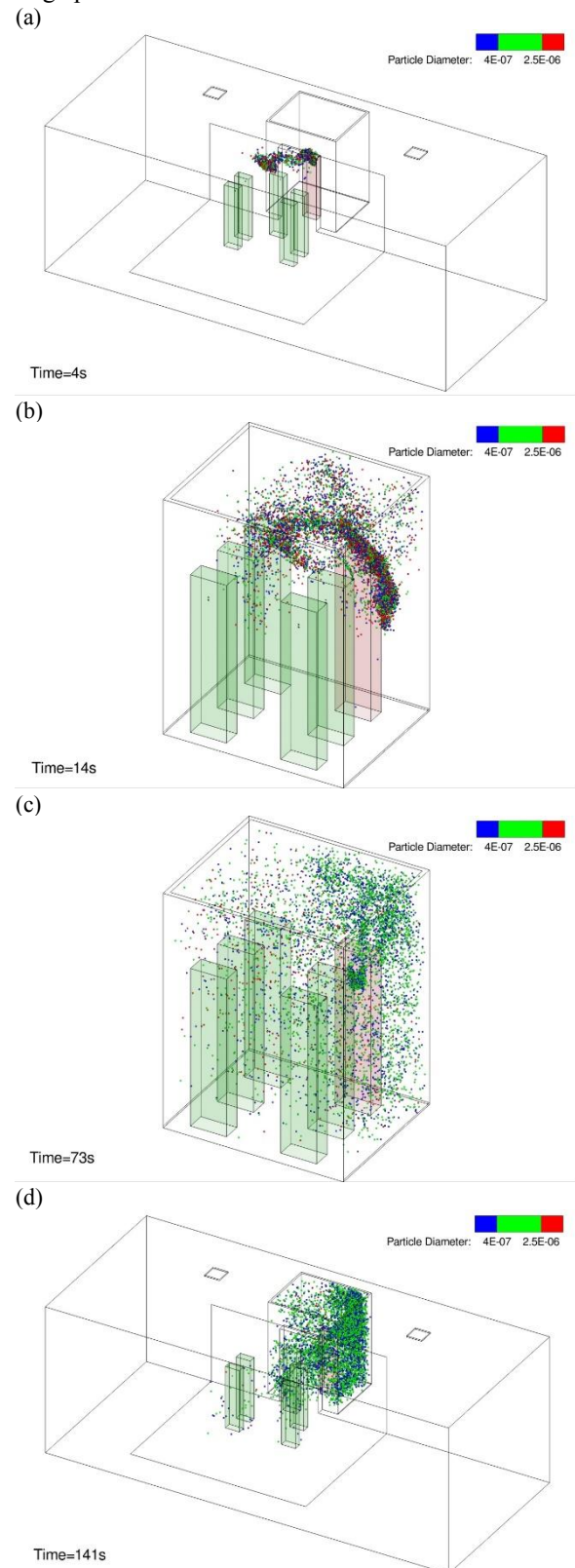
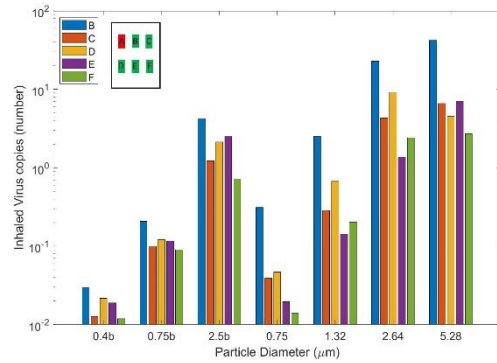


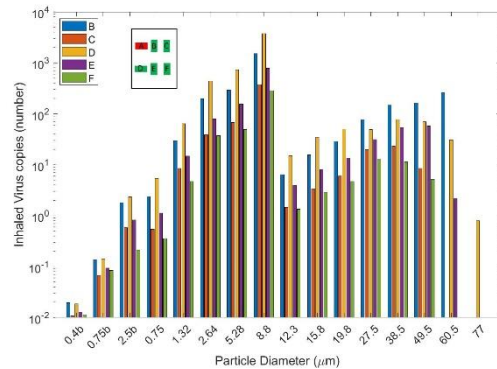
Fig. 3. Transient particle dispersion of Case 1 (unit: m)

3.2 Size distribution of inhaled particles

As particle size plays an important role in the particle transmission and the number of virus copies carried, information about the size distribution of inhaled particles is helpful in determining potential intervention methods. For example, this information can guide decisions about whether to increase social distancing. Large particles contain many more copies of a virus than small particles but fall to the ground very quickly, whereas small particles can travel further and remain suspended for a longer time. Fig. 4 shows the size distribution of particles with respect to the number of inhaled virus copies during the two-minute elevator ride. The subscript “b”, as in “0.4b” and “0.75b” on the x-axis, indicates that the particles were generated by breathing (injected from the nose). Those x-values without a subscript indicate that the particles were from other activities like speaking or coughing (injected from the mouth). The results show that the majority of the inhaled virus copies were from particles with a nucleus diameter less than $10 \mu\text{m}$, which agrees with the findings of Chen et al. [27]. No particles with a diameter greater than $77 \mu\text{m}$ was found in the breathing zones of susceptible passengers. As the traveling ability of larger particles was more limited than that of smaller particles, a larger number of virus copies inhaled were observed from passengers with closer proximity to the index person.

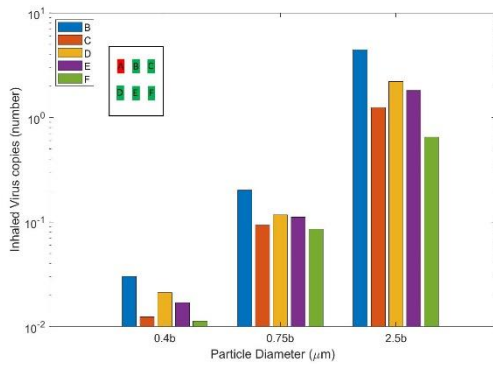


(c) Size distribution of particles inhaled by susceptible passengers in the covered coughing case (Case 3)

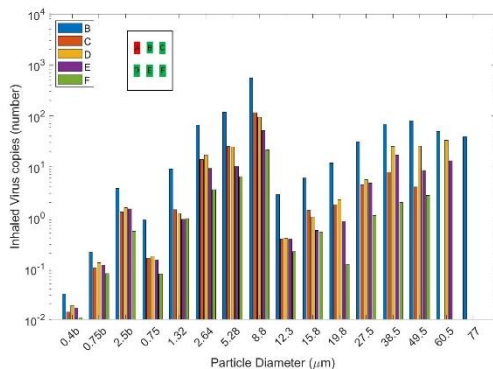


(d) Size distribution of particles inhaled by susceptible passengers in the speaking case (Case 4)

Fig. 4. Size distribution of inhaled virus-laden particles



(a) Size distribution of particles inhaled by susceptible passengers in the breathing case (Case 1)

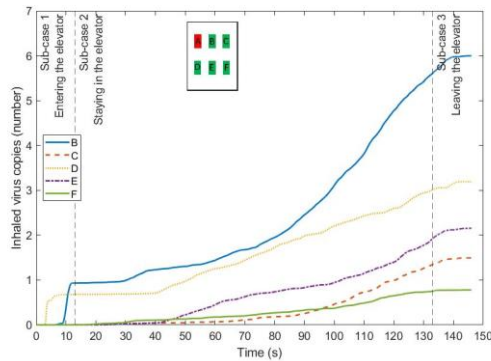


(b) Size distribution of particles inhaled by susceptible passengers in the uncovered coughing case (Case 2)

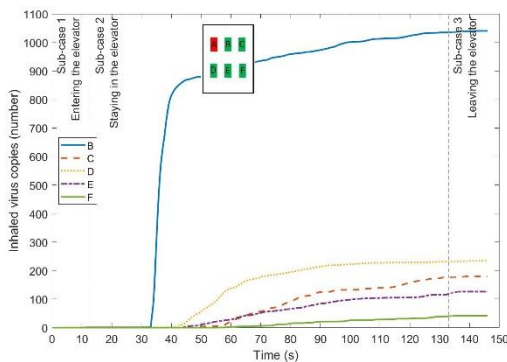
3.3 Virus copies inhaled by fellow passengers during different respiratory activities

The infection risk for each susceptible passenger was estimated by counting the number of virus copies inhaled. Fig. 5 shows the cumulative number of virus copies inhaled by different passengers in the elevator. One can compare the infection risks for the five susceptible passengers. In the breathing case (Case 1), the number of virus copies inhaled by all susceptible passengers was low and nearly negligible, even though a two-minute elevator ride plus 26 seconds of walking in close proximity to the infected person would intuitively be considered dangerous. In the uncovered coughing case (Case 2), one-time coughing occurred at $t = 33 \text{ s}$ (20 s after entering the cabin). A sharp increase in the virus dose for passenger B was observed immediately after the coughing. The increased virus dose for the other passengers neatly followed the order of their distance from the index person; the observed increase in virus dose occurred later for passengers further from the index person. The covered coughing case (Case 3) exhibited the same trend as Case 2, but the infection risks for all susceptible passengers were significantly lower, as the coughing jet was suppressed, and large particles were filtered out by the mask. In the speaking case (Case 4), the face directions of the index person and passenger D changed, because this study assumed that they were having a face-to-face conversation during the elevator ride. In total, the index

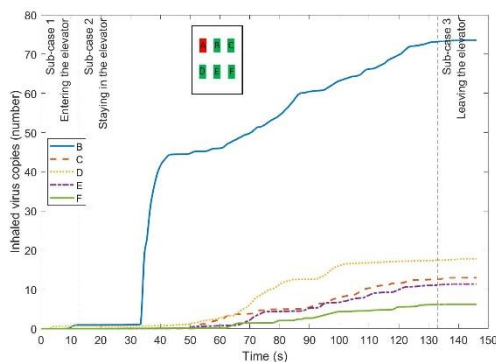
person spoke for 60 seconds during the 2-minute ride. The infection risks for all susceptible passengers were relatively high because of the continuous particle injection. However, differently from Case 2, no sudden increase in particle inhalation was observed immediately after the speaking activity began. Overall, the susceptible passengers who were downstream from the index person faced the highest infection risk. Passengers B and D would be infected with COVID-19.



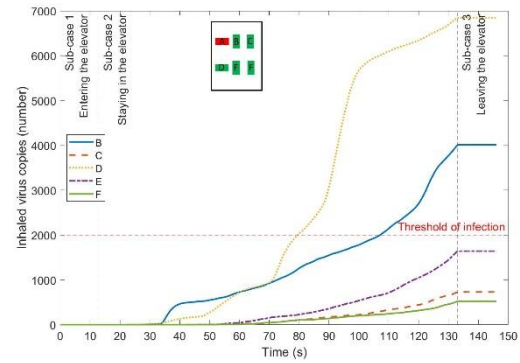
(a) Infection risk for susceptible passengers in the breathing case (Case 1)



(b) Infection risk for susceptible passengers in the uncovered coughing case (Case 2)



(c) Infection risk for susceptible passengers in the covered coughing case (Case 3)



(d) Infection risk for susceptible passengers in the speaking case (Case 4)

Fig. 5. Assessment of the infection risk during the elevator ride with different respiratory activities

4 Discussion

4.1 Effects of different activities

To quantitatively compare the infection risks of different respiratory activities, this study investigated four typical elevator ride scenarios. The number of inhaled virus copies during a complete elevator ride for each passenger is shown in Table 3. If the index person's only respiratory activity during the ride was breathing, the amount of virus intake by other passengers would be very low in comparison to the estimated 2,000-copy threshold for infection risk. The trend that the passengers closer to the index person had a higher virus intake suggests the effectiveness of distancing, even for small airborne particles. Distancing also reduces the exposure to larger particles, as they have a shorter transport range. The virus intake by fellow passengers can be reduced to only 7% to 15% if the index person covers his/her mouth while coughing. Meanwhile, the results indicate a much higher infection risk in the talking case. The two passengers closest to the index person were at the greatest risk of infection, as the viral dose exceeded the threshold. The talking case demonstrates the importance of orientation, as downstream passengers faced the highest infection risk. Overall, the activity of breathing can be considered insignificant when coughing or speaking activities are present.

Table 3. Summary of inhaled SARS-COV-2 virus copies for different respiratory activities by the index person

Passenger	B	C	D	E	F
Breathing	6.0	1.5	3.2	2.2	0.8
Uncovered coughing	1040.3	179.4	234.4	126.4	41.7
Covered coughing	73.6	13.0	17.8	11.4	6.2
Speaking	4011.0	728.2	6848.0	1640.5	521.7

Compared to a related study [22] in which infection risks for fellow passengers were high, this study found

relatively low infection risks during a typical elevator ride. This was mainly because of the short duration of the ride. The intensity of viral exposure for a certain period was still considerable. Furthermore, the high air change rate could alleviate the infection risk. According to ASHRAE standards [25, 26], an air change rate of only 3 or 4 times per hour is sufficient for offices, and it is about one-eighteenth of the air change rate in the present study. The risk can be further reduced if susceptible passengers wear masks.

4.2 Limitation and future work

The RANS model with the RNG $k-\epsilon$ turbulence model was used for numerical simulation. The CFD models were subject to a trade-off between accuracy and computational load. For the discrete phase model, this study assigned an inert property for the virus-laden particles because the evaporation time was short for the range of particle size.

For estimating the infection risk, this study assumed a well-mixed breathing zone. Since the breathing zone was defined as a sphere with a radius of 0.3 meter, it was subject to a non-uniform distribution of particles. Especially for transient cases, clusters of particles can be frequently observed. The use of an averaged particle concentration in a breathing zone can lead to either overestimation or underestimation of the actual risk. However, since the flow field was highly turbulent, this assumption can be valid.

There are many well-recognized studies on the particle size distribution from human activities such as breathing, speaking and coughing [10,11,12]. However, there are still very limited studies on the viral loads in each size range of emitted particles (i.e., live virus concentration in terms of copies/mL). The uncertainty level of the results for virus copies inhaled (Section 3.3) can be significantly higher than that for size distribution of inhaled particle (Section 3.2). Due to the limited availability of information about SARS-COV-2 virus-laden particles that originate from the human respiratory system, a high viral load from the clinical studies was chosen in this research. The viral load concentration was further assumed to be uniform regardless of the size distribution of inhaled particles. The viral load results presented by the clinical studies were the probabilities of virus presence in particles. This study averaged the viral load for all particles, assuming that the statistical mean was able to represent the infection risk.

Moreover, SARS-COV-2 has evolved, and many variants have been identified and reported by the CDC. The Omicron variant, as the dominant strain of the virus circulating around the world, is less severe in general than earlier reported variants such as Alpha, Beta and Delta [28]. However, the Omicron variant has been reported to be more contagious, which is believed to have resulted from immune evasion [29]. Such facts may lead to a different quantum of infection, and the threshold of 2,000 inhaled virus copies from earlier COVID-19 studies may already be outdated.

Also, passengers may get in or leave the elevator cabin during the ride. Different riding times can lead to different levels of exposure to viruses for susceptible

passengers. Passengers' face orientations may vary as well. In addition, combinations of respiratory activities may occur. These variations can greatly affect the particle transmission. However, qualitative conclusions presented in this study should still be valid.

This study used a mixing ventilation system with air blown into the cabin from the periphery of the ceiling. The reasonably high ventilation rate caused the particles to be well mixed in the elevator space. If other types of ventilation were employed, such as a displacement ventilation system or personalized ventilation system, stratifications or non-uniform distributions of particles could be expected. An appropriate ventilation system design has considerable potential to reduce the infection risk for the non-index passengers.

5 Conclusion

This study used a CFD model with particle dispersion to estimate the infection risks for susceptible passengers in an elevator ride. The study led to the following conclusions:

- Particle generation and transmission patterns vary considerably among different respiratory activities. The breathing activity of a SARS-COV-2 infected person releases the fewest virus-laden particles, and fellow passengers may not be infected with COVID-19. When the index person coughs during an elevator ride, covering the cough thoroughly can reduce the virus intake of fellow passengers by 85% to 93%. Among four different scenarios, talking to each other seems the most dangerous in regard to becoming infected with COVID-19. In the talking scenario, it is highly possible that the passengers who are in close proximity to the index person will be infected.
- An elevator cabin is a crowded and confined space that facilitates the transmission of virus-laden particles. The infection risk decreases with the distance from the index person. Thus, social distancing is helpful during elevator rides.

References

1. COVID-19 Map - Johns Hopkins Coronavirus Resource Center. Accessed April 19, 2022. <https://coronavirus.jhu.edu/map.html>
2. Coronavirus (COVID-19) frequently asked questions | CDC. Accessed April 19, 2022. <https://www.cdc.gov/coronavirus/2019-ncov/faq.html>
3. Khanh NC, Thai PQ, Quach HL, et al. Transmission of SARS-CoV 2 during long-haul flight. *Emerg Infect Dis.* 2020;26(11):2617-2624. doi:10.3201/eid2611.203299
4. Chen J, He H, Cheng W, et al. Potential transmission of SARS-CoV-2 on a flight from Singapore to Hangzhou, China: An epidemiological investigation. *Travel Medicine*

- and Infectious Disease*. 2020;36.
doi:10.1016/j.tmaid.2020.101816
5. Xie C, Zhao H, Li K, et al. The evidence of indirect transmission of SARS-CoV-2 reported in Guangzhou, China. *BMC Public Health*. 2020;20(1). doi:10.1186/s12889-020-09296-y
 6. Jin T, Li J, Yang J, et al. SARS-CoV-2 presented in the air of an intensive care unit (ICU). *Sustainable Cities and Society*. 2021;65. doi:10.1016/j.scs.2020.102446
 7. Gupta JK, Lin CH, Chen Q. Characterizing exhaled airflow from breathing and talking. *Indoor Air*. 2010;20(1):31-39. doi:10.1111/j.1600-0668.2009.00623.x
 8. Chen C, Lin CH, Jiang Z, Chen Q. Simplified models for exhaled airflow from a cough with the mouth covered. *Indoor Air*. 2014;24(6):580-591. doi:10.1111/ina.12109
 9. Gupta JK, Lin CH, Chen Q. Flow dynamics and characterization of a cough. *Indoor Air*. 2009;19(6):517-525. doi:10.1111/j.1600-0668.2009.00619.x
 10. Chao CYH, Wan MP, Morawska L, et al. Characterization of expiration air jets and droplet size distributions immediately at the mouth opening. *Journal of Aerosol Science*. 2009;40(2):122-133. doi:10.1016/j.jaerosci.2008.10.003
 11. Fabian P, McDevitt JJ, DeHaan WH, et al. Influenza virus in human exhaled breath: An observational study. *PLoS ONE*. 2008;3(7). doi:10.1371/journal.pone.0002691
 12. Yang S, Lee GWM, Chen CM, Wu CC, Yu KP. The size and concentration of droplets generated by coughing in human subjects. *Journal of Aerosol Medicine: Deposition, Clearance, and Effects in the Lung*. 2007;20(4):484-494. doi:10.1089/jam.2007.0610
 13. Pan Y, Zhang D, Yang P, Poon LLM, Wang Q. Viral load of SARS-CoV-2 in clinical samples. *The Lancet Infectious Diseases*. 2020;20(4):411-412. doi:10.1016/S1473-3099(20)30113-4
 14. To KKW, Tsang OTY, Yip CCY, et al. Consistent detection of 2019 novel coronavirus in saliva. *Clinical Infectious Diseases*. 2020;71(15):841-843. doi:10.1093/cid/ciaa149
 15. Dbouk T, Drikakis D. On airborne virus transmission in elevators and confined spaces. *Physics of Fluids*. 2021;33(1). doi:10.1063/5.0038180
 16. Shao S, Zhou D, He R, et al. Risk assessment of airborne transmission of COVID-19 by asymptomatic individuals under different practical settings. *J Aerosol Sci*. 2021;151:105661. doi:10.1016/j.jaerosci.2020.105661.
 17. Liu S, Zhao X, Nichols SR, et al. Evaluation of airborne particle exposure for riding elevators. *Building and Environment*. 2022;207:108543. doi:10.1016/J.BUILDENV.2021.108543
 18. Yakhot V, Orszag SA, Thangam S, Gatski TB, Speziale CG. Development of turbulence models for shear flows by a double expansion technique. *Physics of Fluids A*. 1992;4(7):1510-1520. doi:10.1063/1.858424
 19. Pope SB. *Turbulent Flows*. Cambridge University Press; 2000. doi:10.1017/CBO9780511840531
 20. Yakhot V, Orszag SA. Renormalization group analysis of turbulence. I. Basic theory. *J Sci Comput*. 1986;1(1):3-51. doi:10.1007/BF01061452
 21. Chen C, Zhao B. Some questions on dispersion of human exhaled droplets in ventilation room: Answers from numerical investigation. *Indoor Air*. 2010;20(2):95-111. doi:10.1111/j.1600-0668.2009.00626.x
 22. Wang W, Wang F, Lai D, Chen Q. Evaluation of SARS-COV-2 transmission and infection in airliner cabins. *Indoor Air*. 2022;32(1). doi:10.1111/ina.12979
 23. Pan J, Harb C, Leng W, Marr LC. Inward and outward effectiveness of cloth masks, a surgical mask, and a face shield. *Aerosol Science and Technology*. 2021;55(6):718-733. doi:10.1080/02786826.2021.1890687
 24. Prentiss M, Chu A, Berggren KK. Superspreading Events Without Superspreaders: Using High Attack Rate Events to Estimate No for Airborne Transmission of COVID-19 Background and Motivation. doi:10.1101/2020.10.21.20216895
 25. American Society of Heating Refrigerating and Air-Conditioning Engineers. ANSI/ASHRAE Standard 62.1-2019. *Ventilation for Acceptable Indoor Air Quality*. Published online 2019.
 26. American Society of Heating Refrigerating and Air-Conditioning Engineers. ANSI/ASHRAE Standard 62.2-2019. *Ventilation and Acceptable Indoor Air Quality in Residential Buildings*. Published online 2019.
 27. Chen W, Zhang N, Wei J, Yen HL, Li Y. Short-range airborne route dominates exposure of respiratory infection during close contact. *Building and Environment*. 2020;176:106859. doi:10.1016/J.BUILDENV.2020.106859
 28. SARS-CoV-2 Variant Classifications and Definitions. Accessed April 25, 2022. <https://www.cdc.gov/coronavirus/2019-ncov/variants/variant-classifications.html>
 29. Cui Z, Liu P, Wang N, et al. Structural and functional characterizations of infectivity and immune evasion of SARS-CoV-2 Omicron. *Cell*. 2022;185(5):860-871.e13. doi:10.1016/J.CELL.2022.01.019
 30. You R, Lin CH, Wei D, Chen Q. Evaluating the commercial airliner cabin environment with different air distribution systems. *Indoor Air*. 2019;29(5):840-853. doi:10.1111/ina.12578